BUILD SIMUL (2017) 10: 229–238
DOI 10.1007/s12273-016-0320-5

Influence of input data on airflow network accuracy in residential buildings with natural wind- and stack-driven ventilation

Krzysztof Arendt [1,2] (✉), Marek Krzaczek[1], Jacek Tejchman[1]

1. Gdańsk University of Technology, Faculty of Civil and Environmental Engineering, 80-233 Gdańsk, Narutowicza 11/12, Poland
2. University of Southern Denmark, Center for Energy Informatics, Odense, Denmark

Abstract

The airflow network (AFN) modeling approach provides an attractive balance between the accuracy and computational demand for naturally ventilated buildings. Its accuracy depends on input parameters such as wind pressure and opening discharge coefficients. In most cases, these parameters are obtained from secondary sources which are solely representative for very simplified buildings, i.e. for buildings without facade details. Although studies comparing wind pressure coefficients or discharge coefficients from different sources exist, the knowledge regarding the effect of input data on AFN is still poor. In this paper, the influence of wind pressure data on the accuracy of a coupled AFN-BES model for a real building with natural wind- and stack-driven ventilation was analyzed. The results of 8 computation cases with different wind pressure data from secondary sources were compared with the measured data. Both the indoor temperatures and the airflow were taken into account. The outcomes indicated that the source of wind pressure data had a significant influence on the model performance.

Keywords

airflow network model,
natural ventilation,
numerical calculations,
pivoted window,
wind pressure

Article History

Received: 4 April 2016
Revised: 27 May 2016
Accepted: 4 August 2016

1 Introduction

Ventilation plays a major part in the indoor environment quality. It is responsible for about the half of heating/cooling loads in well-insulated buildings. Therefore, the ability to accurately assess the ventilation performance is crucial for a building design process. The performance analysis is often performed using the building energy simulation (BES). The most challenging phenomenon to be modelled in BES is airflow in buildings. The wind- and/or stack-driven ventilation types (Freire et al. 2013; Krzaczek et al. 2015; Zhai et al. 2011) are particularly difficult to be captured in calculations. The highly variable wind speed and its direction, opening characteristics, building aerodynamics and building surroundings are the factors which make a modeling process difficult and lead to simplifying assumptions affecting the model accuracy.

Due to the simplicity of the natural ventilation in a multi-chimney configuration, it is still a very common ventilation type in some cold climate zones, e.g. in Poland, and central and eastern Europe. In this ventilation type, the fresh air is supplied through open windows, cracks or air inlet grills. The waste air is exhausted through vertical ducts in chimneys. The ducts are usually located in bathrooms and kitchens. They act as passive stacks and enforce airflow. Under cold climate conditions, the indoor temperature is higher than the outdoor temperature, resulting in the airflowing from inlets to chimney outlets. However, the wind may have a noticeable effect on the airflow, up to causing reversed flow (Gładyszewska-Fiedoruk and Gajewski 2012).

There are several approaches for simulating indoor airflow in buildings. The simplest approach is a schedule-based airflow in which the air volume rate is arbitrarily assumed. The second approach uses empirical or semi-empirical equations (de Gids and Phaff 1982; Larsens 2006). The third one is the airflow network (AFN) model in which a building is represented by zones and linkage elements (windows, doors, cracks etc.) (Feustel 1998; Gu 2007; Feustel

E-mail: krzysztof.arendt@gmail.com

and Rayner-Hooson 1990). The results with a higher accuracy may be obtained using zonal or CFD approaches. In zonal models, momentum effects are simplified by means of power-law equations (Haghighat et al. 2001; Wurtz et al. 2006; Musy et al. 2002) and the indoor space (e.g. room) is divided into several control volumes. In CFD the full Navier-Stokes equations together with mass and energy conservation equations are solved (Zhai et al. 2002; Zhai and Chen 2005; Wang and Wong 2008, 2009; Arendt and Krzaczek 2014) and each zone is discretized using thousands of finite volumes. Due to the significant computational demand, the use of CFD models is limited to single-zone simulations only (Wang and Wong 2009; Gijón-Rivera et al. 2013). The zonal models are not significantly superior when reducing the computing time over coarse-grids in CFD (Chen 2009). However, they are difficult to apply due to the need of special cells in regions where high momentum effects occur (Chen 2009).

Attempts have been made to limit computational needs of CFD-BES coupled models (Arendt and Krzaczek 2014; Jin et al. 2015; Zhang et al. 2013a; Kim et al. 2015) and to use them for simulations of entire buildings (Zhang et al. 2013b; Barbason and Reiter 2014). The most attractive balance between the accuracy and computational demand in simulations of naturally ventilated buildings is provided by the AFN model. The main difficulty in the development of AFN is the need to estimate opening flow characteristics and building wind pressure coefficients. The opening flow characteristics are the discharge coefficient C_d [—] (used for large openings), defined as $Q = C_d A\sqrt{2\Delta P / \rho}$, and the reference air mass flow rate C_Q [kg·s^{-1}·Pa^{-1}] (used for cracks), defined as $Q = C_Q (\Delta P)^n$, wherein Q is the flow rate through the opening [kg·s^{-1}], ΔP denotes the pressure difference between zones [Pa], ρ is the air density [kg·m^{-3}] and n denotes the empirical coefficient (Feustel and Rayner-Hooson 1990). In other words, the discharge coefficient C_d is defined as a ratio of the actual flow to the ideal flow, while the reference air mass flow rate is the mass flow rate for the pressure difference of 1 Pa. Both parameters depend on the opening geometry, air speed, geographical orientation, surrounding buildings, urban morphologies and the target building shape itself (Iqbal et al. 2015; Hult et al. 2012; Jin et al. 2015; Hang and Li 2012). Due to insufficient building-specific test data, the influence of these factors is often neglected in AFN simulations. The discharge coefficient of 0.6 is usually assumed for rectangular openings in simulations (Hult et al. 2012; Heiselberg et al. 2001). However it was reported in some studies that this coefficient might be significantly lower or higher for certain opening types (Krzaczek et al. 2015; Iqbal et al. 2015; Heiselberg et al. 2001).

The wind pressure coefficients describe how the wind affects the external pressure distribution around a building. They depend mainly on the building geometry, facade details, building surroundings, wind speed, wind direction and turbulence intensity (Cóstola et al. 2009). In practice, it is very difficult to determine an accurate relationship between wind pressure coefficients and all these factors. The most realistic approaches are full-scale on-site experiments (Jensen and Franck 1965; Richardson et al. 1990; Levitan et al. 1991; Richards et al. 2001). However, they are expensive and usually the results come with high uncertainties. The estimated data may be obtained from the following sources: a) wind tunnel tests (Belleri et al. 2014; Sun et al. 2008), b) CFD simulations (Montazeri and Blocken 2013), c) analytical models (Grosso 1995; Swami and Chandra 1988) and d) databases (Liddament 1996). The on-site experiments, wind tunnel tests and CFD simulations belong to the primary data sources (Cóstola et al. 2009). The analytical models and databases are the secondary sources (Cóstola et al. 2009) and are used in the majority of studies.

Cóstola et al. (2009) compared wind pressure data from different data sources and found large discrepancies between them, even for simple cases like cubic and fully exposed buildings. The authors concluded that incomplete wind pressure data raises a serious question concerning simulation accuracy. In addition, secondary data sources are available for simple buildings without facade details only. Montazeri and Blocken (2013) analyzed the wind pressure distribution on facades with balconies and showed that facade details highly affected the results. Ramponi et al. (2014) performed a sensitivity analysis on the influence of wind pressure data from different sources on the night ventilation performance in a model building. The building geometry was intentionally kept as simple as possible (no facade details) and the building was solely cross-ventilated. The authors concluded that the ventilation rate differed up to 15% for different wind pressures.

The recent research studies on comparison of wind pressure data from different sources and their influence on the models accuracy are very limited. Moreover, the studies are focused on the simple building geometries, and the results have not been validated by the measurement results.

The aim of the present paper is to study the influence of the wind pressure data from different sources on the accuracy of a coupled AFN-BES model. A real building equipped with a wind- and stack-driven ventilation system is taken as a case study. Eight calculation cases with different wind pressure data based on two secondary sources were taken into account. The resulting indoor airflow and temperatures were compared with the full-scale measurements. A small residential building with available measurements of climate conditions and indoor environment parameters was chosen as a case study.

The innovative point of the present work is the study of the effect of the uncertainty in the wind pressure data on a real building rather than on an idealized one.

2 Test building

The test building is a two-story residential building (Fig. 1) located in Skarszewy, northern Poland (Krzaczek et al. 2015). It was equipped with a natural wind- and stack-driven ventilation system in a multi-chimney configuration. The building was divided into 2 separate, fully functional apartments: one on the ground floor and one on the first floor. The 7-day measurements (June 2013) were taken in the apartment located on the first floor only. The usable area of the test apartment was 86.33 m^2, the ceiling height was 2.62 m and the total volume was 226.18 m^3. The apartment was equipped with 4 vertical chimney air ducts in the bathroom (1 duct), technical room (1 duct) and living room with a kitchen annex (2 ducts) (Fig. 1). The air-duct's cross-section area was 196.0 cm^2 (0.14 m × 0.14 m). The air inlets into the chimney ducts were located 0.15 m below the room ceiling. Each air duct was 1.03 m long. All windows were shaded by overhanging eaves with the depth of 0.8 m. For the study purpose, a single horizontal pivot bottom-hinged window located close to the building's corner was kept open during measurements. The window height was 1.34 m, the width was 0.96 m and the opening angle was 6°. The building components U-values were 1.7 W/(m^2·K) for the windows, 0.161 W/(m^2·K) for the walls and 0.206 W/(m^2·K) for the roof. The solar heat gain coefficient for windows was 0.45.

The measured outdoor parameters included the wind speed and direction, as well as the outdoor air dry-bulb temperature. In the indoor space, the following quantities were measured: indoor air temperature in rooms, air speed and temperature at all the air outlet grills (4 chimneys), and indoor and outdoor barometric pressures. The wind speed and direction were measured at 1.85 m above the roof cover layer. The probe time of 60 s was chosen for the measurements. The window net airflow $V_{w,net}$ (the sum of the inflow and outflow) was derived analytically from the air mass balance in the building, based on the measured airflow in all other openings (outlet grills). Therefore, the infiltration airflow (through unintentional leakages) was included in the derived window airflow. The sensor accuracy was ±0.1 °C for the temperature and ±2.0% for the air speed.

3 Model formulation

The airflow in the test building was modelled with the AFN approach implemented in the program EnergyPlus 8.1 (AFN-BES co-simulation). The AFN equations were described by Walton (1989). The implementation of the airflow network model in EnergyPlus was discussed by Gu (2007). In this section, only the most important equations for this study are summarized. All building partitions were modelled based on the building's technical project. The apartment on the ground floor was not included and an adiabatic surface was assumed along the floor structure mid-plane. The air was assumed to be inviscid and incompressible. The zonal nodes were connected with each other using linkage elements representing equations governing inter-zonal airflow. The equations are semi-empirical in nature and are based on pressure differences on both opening sides. The uniform zone temperatures and hydrostatic pressure distribution were assumed within each zone. The buoyancy-driven flow was solely possible between zones located at different heights (i.e. between a room and chimney).

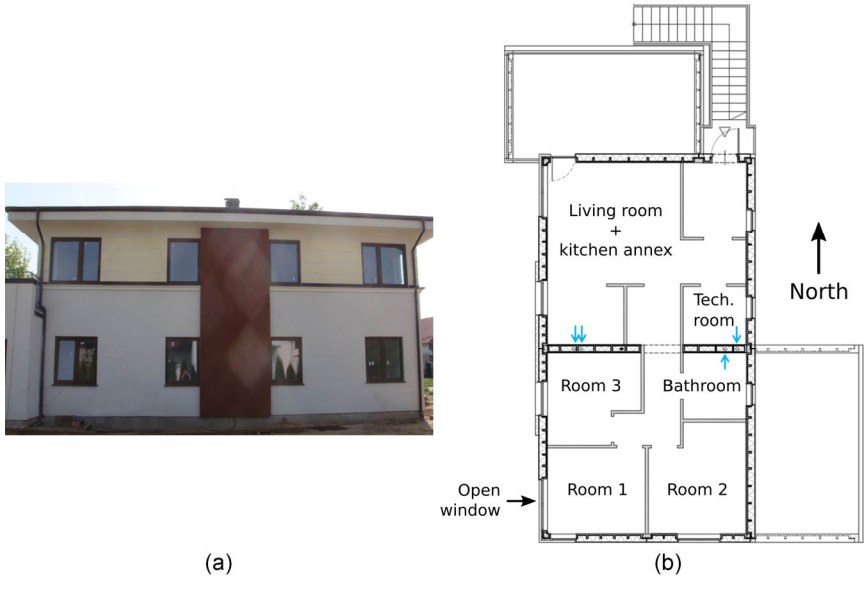

Fig. 1 (a) West facade of test building and (b) 1st floor plan (test apartment) (chimney inlets are marked with blue arrows)

The building model was divided into 2 residential thermal zones: "Z1" and "Z2" (Fig. 2). The zones had identical volumes and were separated by a wall with a large vertical opening (door D: Z1-Z2). The zone "Z1" was equipped with a horizontal pivot bottom-hinged window (W: E0-Z1). The closed windows on each wall were merged.

The EnergyPlus implementation of AFN lacks a linkage equation to simulate passive stacks (air ducts for passive ventilation) like the one implemented in COMIS (Feustel 1998). Thus, the chimney ducts were modelled as standard zones in order to account for the stack effect. Four chimney ducts were modelled by 3 zones "V1", "V2" and "V3". The chimneys were connected with the zones "Z1" and "Z2" and outdoor nodes "E1", "E2" and "E3" using crack linkages. The chimney zone "V3" covered 2 adjacent air ducts in the zone "Z2". The chimney zone surfaces were adiabatic and the heat was exchanged with adjacent zones by convection only.

The net volumetric airflow rate V_{net} [m³/h] in zones was computed based on the net mass flow rate Q_{net} [kg/s] and zone air average density ρ_{air} [kg/m³]:

$$V_{net} = 3600\frac{Q_{net}}{\rho_{air}} \tag{1}$$

The zone net mass flow rate Q_{net} [kg/s] was determined by summing all mass flow rates $Q_{ext,i}$ [kg/s] through the zone's external openings:

$$Q_{net} = \sum_i Q_{ext,i} \tag{2}$$

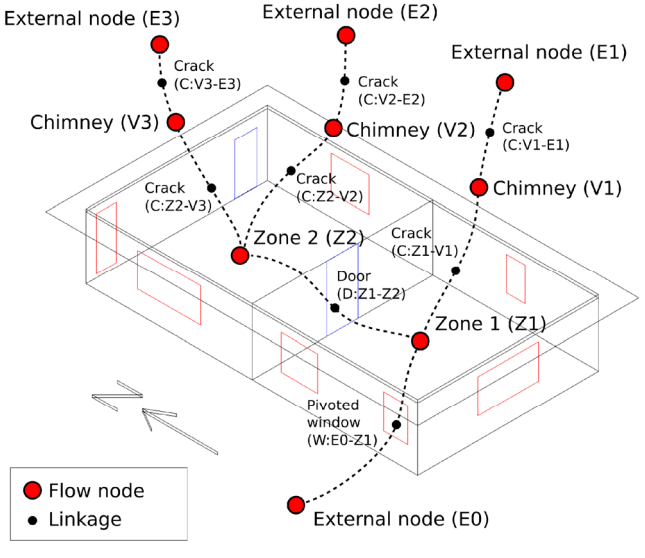

Fig. 2 Model geometry and airflow network topology (chimney zone outlines are not included)

The window net mass flow rate $Q_{w,net}$ [kg/s] was calculated as follows:

$$Q_{w,net} = C_d \int_{z=0}^{z=H} \rho v(z) W dz \tag{3}$$

where $v(z)$ is the air velocity [m/s] as the function of the height z [m] and W is the opening width [m]. Since the window was bottom-hinged, the effective width W_{piv} was calculated (EnergyPlus, DOE 2013):

$$W_{piv} = \sqrt{\frac{1}{\frac{1}{W^2} + \frac{1}{(-2z\tan\alpha)^2}}} \tag{4}$$

where α is the opening angle [°]. The air velocity $v(z)$ in large vertical openings (window and door) was calculated as follows (DOE 2013):

$$v(z) = C_d\sqrt{2\frac{P_{E0}(z) - P_{Z1}(z)}{\rho}} \tag{5}$$

where C_d is the opening discharge coefficient [—], P_{E0} —the pressure vertical distribution [Pa] for the node "E0", P_{Z1}— the pressure vertical distribution [Pa] at the node "Z1" and ρ— the air density [kg/m³]. Finally, the airflow through cracks Q_{cr} [kg/s] was calculated from a simple power law equation (Feustel and Rayner-Hooson 1990):

$$Q_{cr} = C_Q(\Delta P)^n \tag{6}$$

where C_Q denotes the reference air mass flow coefficient [kg·s^{-1}·Pa^{-1}] and n is the empirical coefficient (assumed as 1).

4 Calculation cases

The simulation analyses include 8 cases (Table 1). The aim of the selected cases was to present the influence of wind pressure data source on the result accuracy. Therefore,

Table 1 Description of calculation cases

Case symbol	Source of wind pressure coefficients	Surrounding characteristics assumed	Modification of wind pressure coefficient C_{p180}
CPC-1	CPCALC+	PAD = 1%	Original
CPC-10	CPCALC+	PAD = 10%	Original
CPC-20	CPCALC+	PAD = 20%	Original
AIVC-flt	AIVC	Flat	Original
AIVC-sct	AIVC	Scattered	Original
CPC-1*	CPCALC+	PAD = 1%	Modified (−0.1)
CPC-10*	CPCALC+	PAD = 10%	Modified (−0.1)
CPC-20*	CPCALC+	PAD = 20%	Modified (−0.1)

the wind pressure data were the only input data varying between the cases. The cases "CPC-1", "CPC-10", "CPC-20", "AIVC-flt" and "AIVC-sct" were the basic models developed based on the available secondary data. The modified cases "CPC-1*", "CPC-10*" and "CPC-20*" were derived from the cases "CPC-1", "CPC-10" and "CPC-20", respectively.

Two wind pressure data sources were taken into account: CPCALC+ generated data (Grosso 1995) ("CPC-1", "CPC-10", "CPC-20") and AIVC data (Liddament 1996) ("AIVC-flt", "AIVC-sct"). CPCALC+ is a program calculating wind pressure coefficients on building envelopes based on reference wind tunnel data, which was developed within the European Research Programme PASCOOL (Grosso 1992, 1993, 1995). The AIVC (Air Infiltration and Ventilation Centre) database is a tabular compilation of wind-tunnel data published in several reports, e.g. in the AIVC workshop proceedings (AIVC 1984). A detailed comparison between these databases was presented by Cóstola et al. (2009). The data provided by these sources significantly varied for the given building (Fig. 3). The AIVC data provided significantly higher wind pressure coefficients for the roof. The highest ratio of the AIVC coefficients to the CPCALC+ coefficients for the roof was 55.6, while the average ratio was 39.3 (Figs. 3(b) and (c)). However, the AIVC coefficients for the window were lower than the CPCALC+ coefficients by the average factor of 2 (Fig. 3(a)).

The CPCALC+ data took into account a non-uniform pressure distribution on the surface while the AIVC data was surface-averaged. The window center point was chosen for the CPCALC+ analysis. The effect of surroundings (wind shields) was captured in CPCALC+ by the plan area density PAD [%] defined as PAD=$A_b/A_t \times 100\%$, where A_b is the built area and A_t is the total area. In the case study it was difficult to estimate the plan area density of building surroundings due to their non-uniformity (neighboring buildings with different sizes and distances and a flat field from the north). Hence, the different plan area densities were considered (Table 1): 1% ("CPC-1"), 10% ("CPC-10") and 20% ("CPC-20").

The AIVC data was provided in a tabular form for different surrounding types: a) open flat area ("AIVC-flt") and b) country with scattered windbreaks ("AIVC-sct"). Neither data source included the effect of facade details as overhanging eaves. The wind pressure coefficients for chimney outlets were assumed to be equal to coefficients for the roof surface because no data were available for such a complex geometry. The cases "CPC-1*", "CPC-10*" and "CPC-20*" had the modified wind pressure coefficient C_{p180} for the wind direction of 180° (Table 1) which was one of the dominant directions (Fig. 4). The modified coefficient ($C_{p180} = -0.1$) was arbitrarily chosen to show the result influence. In all cases the window discharge coefficient C_d=0.6 was assumed, often adopted for large openings (Iqbal et al. 2015; Hult et al. 2012; Heiselberg et al. 2001).

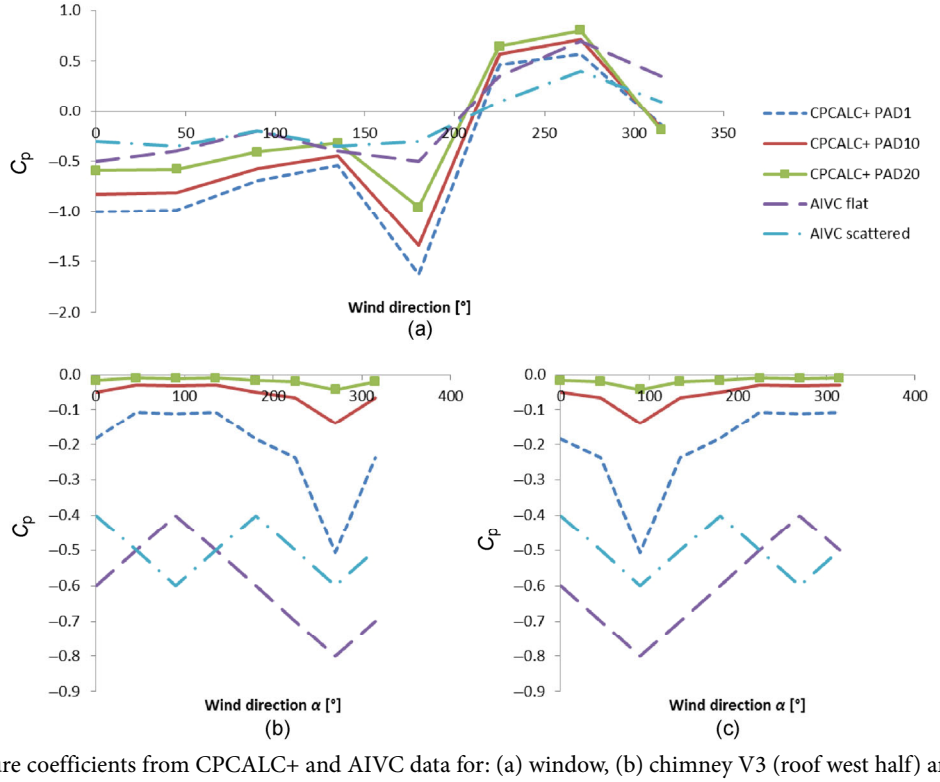

Fig. 3 Wind pressure coefficients from CPCALC+ and AIVC data for: (a) window, (b) chimney V3 (roof west half) and (c) chimneys V1 and V2 (roof eastern half)

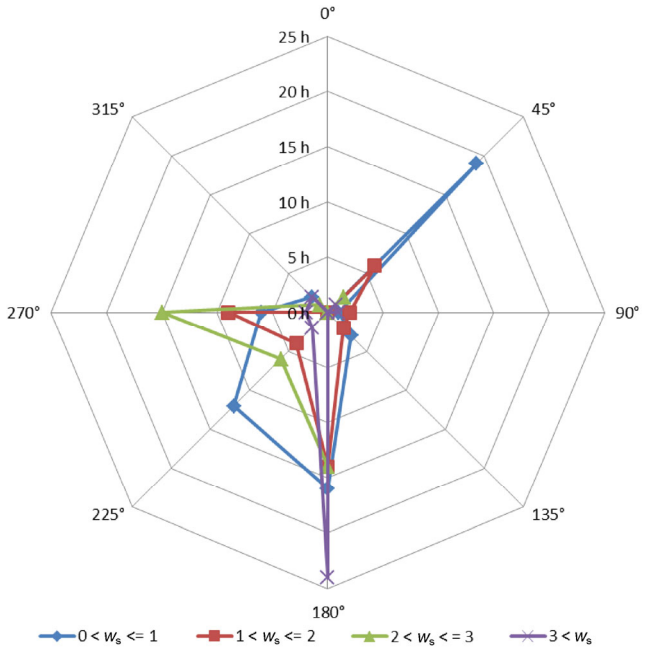

Fig. 4 Wind rose diagram showing total time [h] and speed w_s [m/s] of wind blowing from each direction [°]

The reference air mass flow coefficients C_Q used in the chimney linkage elements (Eq. (6)) were calibrated based on the measured pressure differences and chimney airflow during the measurement time-period. The C_Q coefficients were 0.15 kg·s^{-1}·Pa^{-1} for "V1" and "V2" and 0.3 kg·s^{-1}·Pa^{-1} for "V3". The C_Q coefficient for the chimney "V3" was assumed to be higher because it was used to model the airflow through two adjacent ducts instead of one.

In all cases, the simulation time-period was the same as the period in which measurements were taken, i.e. from June 10, 12:00 p.m. to June 17, 12:00 p.m. Since measurements for the preceding period were not available, the building thermal inertia effects in the initial period were not accurate. Therefore, the model accuracy was solely assessed for the period from June 13, 12:00 to June 17, 12:00 (three initial days were excluded). The outdoor dry-bulb temperature, wind speed and direction in simulations were based on measurements. The solar radiation was based on the Typical Meteorological Year due to unavailable measured data for this parameter.

5 Results and discussion

The accuracy of each case was quantified by the mean absolute error and mean relative error defined as follows:

$$\mathrm{MAE}(X) = \frac{1}{t_{\mathrm{end}}} \int_0^{t_{\mathrm{end}}} \left| X_{\mathrm{m}}(t) - X_{\mathrm{s}}(t) \right| \mathrm{d}t \tag{7}$$

and

$$\mathrm{MRE}(X) = \frac{\bar{X}_{\mathrm{m}} - \bar{X}_{\mathrm{s}}}{\bar{X}_{\mathrm{m}}} \times 100\% \tag{8}$$

where MAE(X) is the mean absolute error of the predicted time-dependent function X, MRE(X) is the mean relative error of the predicted function X, t_{end} is the time period [s], $X_{\mathrm{m}}(t)$ is the measured result for X as the function of the time t, X_{s}(t) is the simulation result for X as the function of the time t and $\bar{X}_{\mathrm{m}}$, $\bar{X}_{\mathrm{s}}$ are the average measured and simulated values during the considered time period. Unlike the mean absolute error, the mean relative error was calculated directly from the average values to neglect small temporal oscillations around the mean value in the measured data. Both error definitions were used to analyze the net volumetric flow rates (MAE(V) and MRE(V)) and indoor temperatures (MAE(T) and MRE(T)).

It was found that there were significant differences in the accuracy of different cases. The most accurate cases as compared to the measurements data were "AIVC-sct" and "CPC-1*", while the case "CPC-1" was the least realistic. The cases "AIVC-sct" and "CPC-1*" had the lowest mean absolute error MAE(V) in the zone volumetric net flow (below 25 m^3/h) (Fig. 5). The lowest mean relative error was obtained in the case "CPC-1*" with MRE(V)=10%. The mean absolute error MAE(V) for the least realistic case "CPC-1" exceeded 120 m^3/h (the corresponding MRE(V) for this case was 169%). It might seem surprising that the most accurate cases ("AIVC-sct" and "CPC-1*") were only around 5 times more accurate than the worst case ("CPC-1"), while the relative change in the associated wind pressure coefficients for the roof was significantly higher (up to 55 times) (Figs. 3(b) and (c)). However, the total opening area of chimneys was about the half of the effective window opening area and the absolute values of the CPCALC+ coefficients were lower than the AIVC coefficients for the roof, but higher for the window (Fig. 3(a)). In all cases MAE(V) was similar for the both zones "Z1" and "Z2"

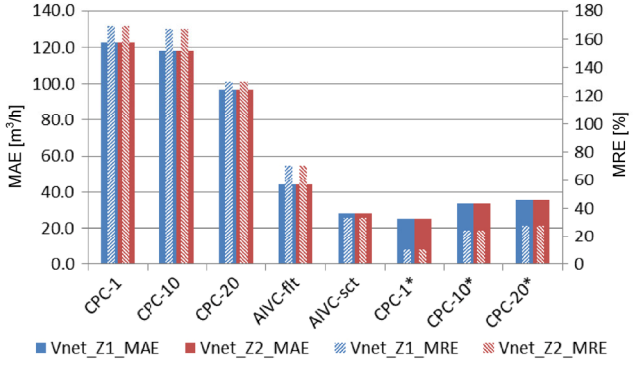

Fig. 5 Mean absolute error MAE(V) and mean relative error MRE(V) of net volumetric flow rate V_{net} [m^3/h] in zones "Z1" and "Z2" for period: June 13, 12:00 – June 17, 12:00

(differences below 0.01 m³/h), indicating that the infiltration through unintentional leakage areas was insignificant. The mean absolute and relative errors in the cases "CPC-1", "CPC-10" and "CPC-20" were significantly higher than in the cases "AIVC-flt" and "AIVC-sct" (Fig. 5). It was surprising because the CPCALC+ data took into account the exact opening location while the AIVC data were surface-averaged.

In the analyzed building, the window was located close to the building's corner, thus the wind pressure coefficients C_p obtained from CPCALC+ and AIVC were significantly different. For the window, the highest difference in wind pressure data was found for the wind direction of w_{dir}=180° (Fig. 3). The measurement results showed that the wind was blowing from this direction for the total time of 68 h and during over one-third of the time the wind speed was above 3 m/s (Fig. 4). This wind direction was parallel to the window surface and created a low-pressure area near the window. In fact, the ventilation rate and temperature results in "CPC-1", "CPC-10" and "CPC-20" were the most inaccurate for w_{dir}=180° (compare Fig. 6 and Figs. 9(a) and (b)). During June 13th, 14th and 15th the measured net volumetric flow rate in the zone "Z1" was positive (meaning infiltration), but the results obtained in "CPC-1"–"CPC-20" were negative (exfiltration) for the wind blowing from the south. On the other hand, the wind pressure coefficients C_{p180} in "AIVC-flt" and "AIVC-sct" were closer to zero and the net flow rate was significantly closer to the reality. It can be concluded that the southern wind did not create such a low pressure around the window as predicted by CPCALC+ in the analyzed building. It should be noted, that this conclusion does not question the validity of the CPCALC+ data but it shows that the data may not be accurate enough in some real cases with unknown disturbances (non-ideal geometry, non-ideal surroundings). The modification of the single wind pressure coefficient C_{p180} to −0.1 in the cases "CPC-1*", "CPC-10*" and "CPC-20*" significantly improved the airflow prediction (Fig. 7). After the correction of C_{p180}, the case "CPC-1" (which was the least accurate) became one of the most realistic ("CPC-1*"). It shows how sensitive the model was to the wind pressure data.

The best agreement with respect to the temperature results was obtained for "AIVC-sct" and "CPC-1*" (MAE(T) below 0.5 °C and MRE(T) below 2%) (Fig. 8). The worst accuracy was found in the cases based on the unmodified CPCALC+ data, i.e. "CPC-1", "CPC-10" and "CPC-20"

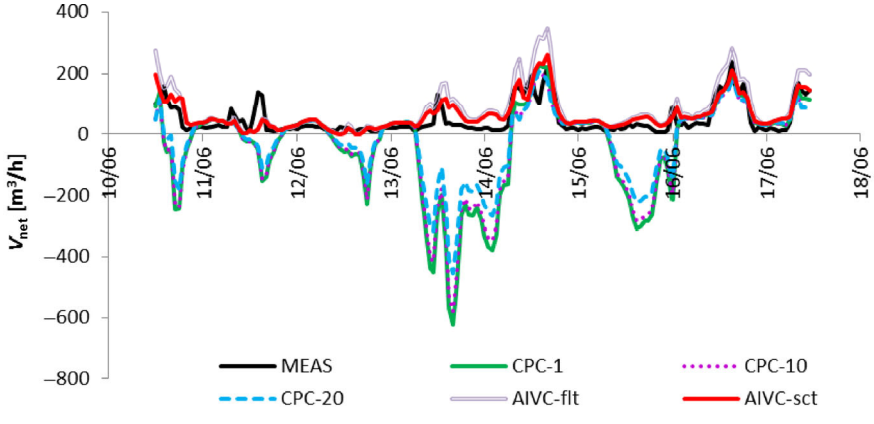

Fig. 6 Net volumetric flow rate $V_{net,Z1}$ in zone "Z1" for cases "CPC-1", "CPC-10", "CPC-20", "AIVC-flt" and "AIVC-sct" versus measured data (MEAS)

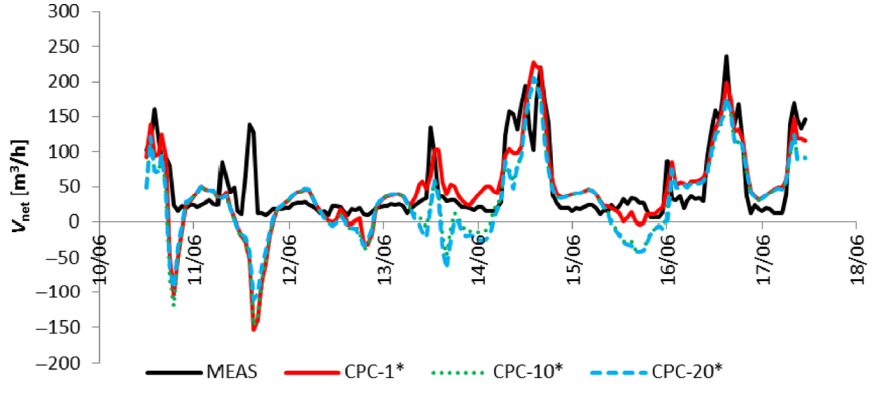

Fig. 7 Net volumetric flow rate $V_{net,Z1}$ in zone "Z1" for cases "CPC-1*", "CPC-10*", "CPC-20*" versus measured data (MEAS)

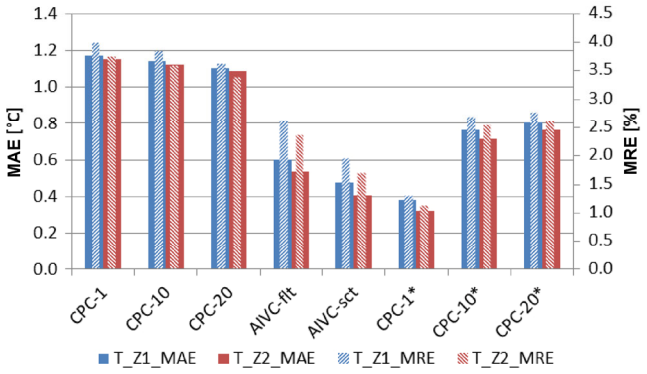

Fig. 8 Mean absolute error MAE(T) and mean relative error MRE(T) of indoor temperature T [°C] in zones "Z1" and "Z2" for period: June 13, 12:00 – June 17, 12:00

(MAE(T) between 1.1 °C and 1.2 °C, MRE(T) between 3.5% and 4.0%). The correlation between the airflow relative accuracy (Fig. 5) and temperature accuracy (Fig. 8) was not linear due to the temperature dependency of the airflow pattern and outdoor air temperature.

The indoor air temperature for "AIVC-sct" and "CPC-1*" closely followed the measured temperature during the last 4 days of the measurement time-period (Fig. 9(a))—the error was within 1°C. With respect to the model simplicity, this accuracy was satisfactory. The significant temperature mismatch in the first 2–3 days of the measurement time-period was caused by inaccurate initial condition and thermal inertia of the building structure. The temperature results for the rest of the measurement time-period suggested that both the heat transmission and infiltration rate were correctly calculated. On the other hand, the indoor air temperature for the case "CPC-1" was inaccurate during the periods with the wind direction around 180° (Figs. 9(a) and (b)). When the wind direction deviated from 180°, the model quickly restored its accuracy. A modification of a single wind pressure coefficient for the dominant wind direction 180° (Fig. 4) significantly increased the temperature accuracy for "CPC-1*" (Fig. 9(a)). The explanation of the model behavior (quick accuracy restoration) during periods when the wind changed its direction from 180° was the reduced stack effect. During the analyzed time-period there was a low temperature difference between the indoor and outdoor air. The average outdoor air temperature during the considered time-period was 17.72 °C while the average indoor air temperature was 22.44 °C. Under such conditions the main driving force for ventilation was the wind, so consequently the wind pressure data had a prevailing effect on the accuracy.

The results obtained based on the AIVC and CPCALC+ wind pressure data differed significantly. Like in most engineering cases, actual wind pressure coefficients for the considered building were unavailable. Based on the

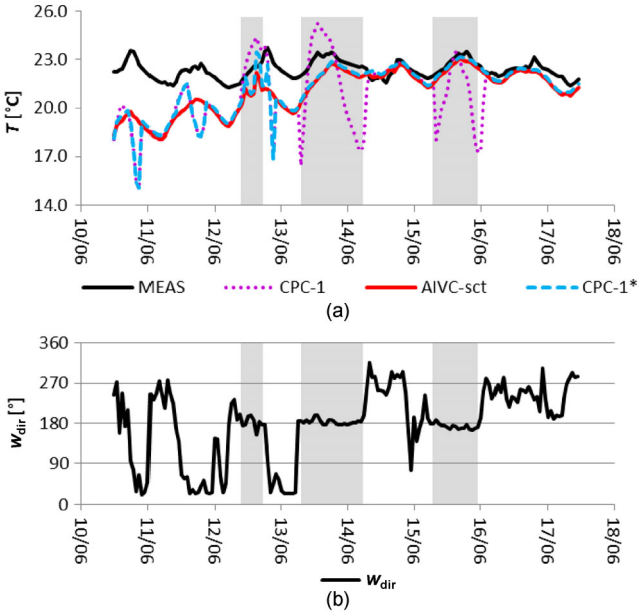

Fig. 9 Temperature variation T [°C] in zone "Z1" in cases "CPC-1", "AIVC-sct" and "CPC-1*" versus measured temperature (MEAS) (a) and wind direction w_{dir} [°] (b) (periods with w_{dir}≈180° are shaded in grey)

simulations results, it can only be presumed that the actual wind pressure coefficients were close to the case "CPC-1*" or "AIVC-sct". However, these cases are not identical (Table 1, Fig. 3). Despite of the differences in the wind pressure data between "CPC-1*" and "AIVC-sct" the simulations results were similar. Hence, more precise estimates of the wind pressure data were impossible. The model and chosen wind pressure data validity can only be ensured for the measurement time-period. The final conclusion is that the AFN simulations at the early design stage, when no extensive experimental data is available for the model validation, are characterized with a significant uncertainty. Therefore, if the model cannot be fully validated, at least comparative simulations based on various wind pressure data are recommended.

6 Conclusions

The study was aimed to analyze the influence of wind pressure data on the accuracy of the coupled AFN-BES model. The model was used to simulate indoor airflow in a naturally wind- and stack-driven ventilated building with multi-chimneys. The simulation results of 8 cases with different wind pressure data from secondary sources were compared with the full-scale measurement results. The simulations were performed for a 7-day long time-period during the late spring. Based on the comparison between simulations and measurements, the following conclusions may be formulated:

1) the wind pressure data source had a significant influence on the model accuracy,
2) the surface-averaged AIVC data (cases "AIVC-flt" and "AIVC-sct"—airflow mean relative errors between 33% and 70%) resulted in the higher accuracy than the unmodified CPCALC+ data (cases "CPC-1", "CPC-10" and "CPC-20" —mean relative errors between 130% and 169%),
3) the modification of a single wind pressure coefficient for one of the dominant wind directions in the case "CPC-1" reduced the mean relative error from 169% down to 10% (case "CPC-1*"), making the least accurate case the most accurate one,
4) the wind pressure data from secondary sources is given for idealized buildings and it might significantly differ, therefore comparative simulations based on data from different sources are recommended in real cases,
5) the application of more complex algorithms in order to obtain wind pressure coefficients (e.g. CPCALC+ over AIVC) does not necessarily improve the overall simulation accuracy in real cases.

Acknowledgements

The present study was supported by the research project "Innovative complex system solution for energy-saving residential buildings of a high comfort class in a unique prefabricated technology and assembly of composite panels" financed by the Polish National Centre for Research and Development NCBR (NR.R1/INNOTECH-K1/IN1/59/155026/NCBR/12).

References

AIVC (1984). Wind Pressure Workshop Proceedings AIC-TN-13.1-84, AIVC, Brussels.

Arendt K, Krzaczek M (2014). Co-simulation strategy of transient CFD and heat transfer in building envelope based on calibrated heat transfer coefficients. *International Journal of Thermal Sciences,* 85: 1–11.

Barbason M, Reiter S (2014). Coupling building energy simulation and computational fluid dynamics: Application to a two-storey house in a temperate climate. *Building and Environment,* 75: 30–39.

Belleri A, Lollini R, Dutton SM (2014). Natural ventilation design: An analysis of predicted and measured performance. *Building and Environment,* 81: 123–138.

Chen Q (2009). Ventilation performance prediction for buildings: A method overview and recent applications. *Building and Environment,* 44: 848–858.

Cóstola D, Blocken B, Hensen JLM (2009). Overview of pressure coefficient data in building energy simulation and airflow network programs. *Building and Environment,* 44: 2027–2036.

de Gids W, Phaff H (1982). Ventilation rates and energy consumption due to open windows: A brief overview of research in the Netherlands. In: Proceedings of erd IEA Air Infiltration Conference.

DOE (2013). EnergyPlus 8.1, Engineering Reference. U.S. Department of Energy.

Feustel HE, Rayner-Hooson A (1990). COMIS Fundamentals. Lawrence Berkeley Laboratory, USA.

Feustel HE (1998). COMIS—An International Multizone Air-Flow and Contaminant Transport Model. Lawrence Berkeley National Laboratory, USA.

Freire RZ, Abadie MO, Mendes N (2013). On the improvement of natural ventilation models. *Energy and Buildings, 62*: 222–229.

Gijón-Rivera M, Xamán J, Álvarez G, Serrano-Arellano J (2013). Coupling CFD-BES Simulation of a glazed office with different types of windows in Mexico City. *Building and Environment,* 68: 22–34.

Gładyszewska-Fiedoruk K, Gajewski A (2012). Effect of wind on stack ventilation performance. *Energy and Buildings,* 51: 242–247.

Grosso M (1992). Wind pressure distribution around buildings—A parametrized model. *Energy and Buildings,* 18, 101–131.

Grosso M (1993). Modelling wind pressure distribution on buildings for passive cooling. In: Proceedings of 3rd European Conference on Architecture: Solar Energy in Architecture and Urban Planning, Florence, Italy.

Grosso M (1995). CPCALC+, Calculation of wind pressure coefficients on buildings, User's manual. Pascool Research Programme, Turin, Itally.

Gu L (2007). Airflow network modeling in EnergyPlus. In: Proceedings of 10th International IBPSA Building Simulation Conference, Beijing, China.

Haghighat F, Li Y, Megri AC (2001). Development and validation of a zonal model—POMA. *Building and Environment,* 36: 1039–1047.

Hang J, Li Y (2012). Macroscopic simulations of turbulent flows through high-rise building arrays using a porous turbulence model. *Building and Environment,* 49, 41–54.

Heiselberg P, Svidt K, Nielsen PV (2001). Characteristics of airflow from open windows. *Building and Environment,* 36: 859–869.

Hult EL, Iaccarino G, Fischer M (2012). Using CFD simulations to improve the modeling of window discharge coefficients. Paper presented at SimBuild, Madison, USA.

Iqbal A, Afshari A, Wigö H, Heiselberg P (2015). Discharge coefficient of centre-pivot roof windows. *Building and Environment,* 92: 635–643.

Jensen M, Franck N (1965). Model-Scale Tests in Turbulent Wind—Part II Phenomena Dependent on the Velocity Pressure. Copenhagen: The Danish Technical Press.

Jin M, Liu W, Chen Q (2015a). Simulating buoyancy-driven airflow in buildings by coarse-grid fast fluid dynamics. *Building and Environment,* 85: 144–152.

Jin R, Hang J, Liu S, Wei J, Liu Y, Xie J, Sandberg M (2015b). Numerical investigation of wind-driven natural ventilation performance in a multi-storey hospital by coupling indoor and outdoor airflow. *Indoor and Built Environment,* doi: 10.1177/1420326X15595689.

Kim D, Braun JE, Cliff EM, Borggaard JT (2015). Development, validation and application of a coupled reduced-order CFD model for building control applications. *Building and Environment,* 93: 97–111.

Krzaczek M, Florczuk J, Tejchman J (2015). Field investigations of stack ventilation in a residential building with multiple chimneys and tilted window in cold climate. *Energy and Buildings,* 103: 48–61.

Larsen TS (2006). Natural ventilation driven by wind and temperature difference. PhD Thesis, Aalborg University, Denmark.

Levitan ML, Mehta KC, Vann WP, Holmes JD (1991). Field measurements of pressures on the Texas Tech building. *Journal of Wind Engineering & Industrial Aerodynamics,* 38: 227–234.

Liddament MW (1996). A Guide to Energy Efficient Ventilation. Air Infiltration and Ventilation Centre, Coventry, UK.

Montazeri H, Blocken B (2013). CFD simulation of wind-induced pressure coefficients on buildings with and without balconies: Validation and sensitivity analysis. *Building and Environment,* 60: 137–149.

Musy M, Winkelmann F,Wurtz E, Sergent A (2002). Automatically generated zonal models for building air flow simulation: Principles and applications. *Building and Environment,* 37: 873–881.

Ramponi R, Angelotti A, Blocken B (2014). Energy saving potential of night ventilation: Sensitivity to pressure coefficients for different European climates. *Applied Energy,* 123: 185–195.

Richards PJ, Hoxey RP, Short LJ (2001). Wind pressures on a 6 m cube. *Journal of Wind Engineering & Industrial Aerodynamics,* 89: 1553–1564.

Richardson GM, Robertson AP, Hoxey RP, Surry D (1990). Full-scale and model investigations of pressures on an industrial/agricultural building. *Journal of Wind Engineering & Industrial Aerodynamics,* 36: 1053–1062.

Sun Y, Tamura Y, Quan Y, Matsui M (2008). The interference effect of surrounding roughness on wind pressures of rectangular prism. In: Proceedings of BBAA VI International Colloquium on Bluff Bodies Aerodynamics & Applications, Milano, Italy.

Swami MV, Chandra S (1988). Correlations for pressure distribution on buildings and calculation of natural-ventilation airflow. *ASHRAE Transactions,* 94(1): 243–266.

Walton GN (1989). AIRNET—A Computer Program for Building Airflow Network Modelling, NISTIR 89-4072. Gaithersburg, MD, USA: National Institute of Standards and Technology,

Wang L, Wong NH (2008). Coupled simulations for naturally ventilated residential buildings. *Automation in Construction,* 17: 386–398.

Wang L, Wong NH (2009). Coupled simulations for naturally ventilated rooms between building simulation (BS) and computational fluid dynamic (CFD) for better prediction of indoor thermal environment. *Building and Environment,* 44: 95–112.

Wurtz E, Mora L, Inard C (2006). An equation-based simulation environment to investigate fast building simulation. *Building and Environment,* 41: 1571–1583.

Zhai Z, Chen Q, Haves P, Klems JH (2002). On approaches to couple energy simulation and computational fluid dynamics programs. *Building and Environment,* 37: 857–864.

Zhai Z, Chen Q (2005). Performance of coupled building energy and CFD simulations. *Energy and Buildings,* 37: 333–344.

Zhai Z, Johnson MH, Krarti M (2011). Assessment of natural and hybrid ventilation models in whole-building energy simulations. *Energy and Buildings,* 43: 2251–2261.

Zhang W, Hiyama K, Kato S, Ishida Y (2013a). Building energy simulation considering spatial temperature distribution for nonuniform indoor environment. *Building and Environment,* 63: 89–96.

Zhang R, Lam KP, Yao S, Zhang Y (2013b). Coupled EnergyPlus and computational fluid dynamics simulation for natural ventilation. *Building and Environment,* 68: 100–113.